Electron Momentum Distribution in Liquid and Solid Rubidium and Cesium as Determined by Positron Annihilation

JOSE A. ARIAS-LIMONTA AND PAUL G. VARLASHKIN
Louisiana State University, Baton Rouge, Louisiana 70803
(Received 17 July 1969; revised manuscript received 17 September 1969)

The momentum distributions of photons from positrons annihilating in liquid and solid rubidium and cesium and in solid krypton and xenon have been measured. The krypton and xenon data are used to remove the core contributions in rubidium and cesium, respectively. Analysis of the resultant conduction-electron momentum distribution shows that (a) indications of higher-momentum components due to scattering into the second zone appear to be predominately a result of core annihilations and largely disappear when the core contribution is removed, and (b) the free-electron model is reasonably accurate for the liquid as well as the solid metals. The core contributions in rubidium and cesium closely approximate a Gaussian distribution. There is little or no change in the ratio of the broad-to-narrow components upon melting.

INTRODUCTION

USING positron annihilation as a probe to measure the characteristics of electrons in metals, several investigators have indicated that free-electron theory is not adequate to describe the conduction-electron momentum distribution of various liquid metals.[1–9] Change in shape of the narrow component upon melting may be due to the loss of the ordered structure of the periodic lattice; however, in some metals, upon heating the distribution changes prior to melting and undergoes slight additional change thereafter. (A fairly extensive discussion of the situation is given in Refs. 1 and 2.)

We have measured the angular correlation of photons from positrons annihilating in liquid and solid rubdium and cesium. This data, when analyzed after removing the background due to annihilations with core electrons, indicates free-electron behavior in these simple metals in the liquid as well as the solid state. Further, there has been considerable discussion of the possibility of higher-momentum components due to scattering into the second zone.[10–15] Rubidium and cesium data when analyzed without core removal strongly indicate the presence of high-momentum components. However, when the contribution from annihilations with the core electrons is removed, the apparent high-momentum components largely disappear.

Let the coincidence counting rate from the usual long-slit angular correlation apparatus for positron annihilation experiments be denoted by $I_z(\theta)$, where θ is the angle by which annihilation photons deviate from 180°. Stewart[16] has shown that $\rho(k) \propto (1/\theta) \times [dI_z(\theta)/d\theta]$ and $N(k) \propto \theta dI_z(\theta)/d\theta$, where $\rho(k)$ is the probability density and $N(k)$ is the density of states. These relations, however, should be applied only to the conduction electrons, and the contribution from annihilations with the core electrons should be removed before attempting this sort of analysis of the data or serious errors can result.

Because of their simplicity, the alkali metals make ideal test cases. It is necessary , of course, to have data available on core annihilations if the core contribution is to be subtracted prior to further analysis. In the case of the alkali metals, the inert elements provide a logical approximation of the core equivalents of the metals. Stewart *et al.*[17] have previously used neon to remove the core contribution of sodium. Because of positronium formation in the liquefied gases, it is preferable to use data on the inert elements in solid form. Because positron-annihilation angular correlation data on solid krypton and xenon[18] shows no sign of positronium formation (as evidenced by the absence of a narrow component in the momentum distribution), rubidium and cesium were chosen as test cases.

EXPERIMENTAL

Data were taken with a long-slit angular correlation apparatus. Sodium-iodide cylindrical detectors 24 in. long were placed behind horizontal lead slits 500 in. apart. The annihilation target was mounted midway

[1] A. T. Stewart, in *Positron Annihilation*, edited by A. T. Stewart and L. O. Roellig (Academic Press Inc., New York, 1967), p. 17.
[2] J. H. Kusmiss and A. T. Stewart, Advan. Phys. **16**, 471 (1967).
[3] A. T. Stewart, J. H. Kusmiss, and R. H. March, Phys. Rev. **132**, 495 (1963).
[4] J. H. Kusmiss, Ph.D. thesis, University of North Carolina at Chapel Hill, 1965 (unpublished).
[5] R. N. West and N. E. Cusack, in *Positron Annihilation*, edited by A. T. Stewart and L. O. Roellig (Academic Press Inc., New York, 1967), p. 309.
[6] J. D. McGervey, in *Positron Annihilation*, edited by A. T. Stewart and L. O. Roelling (Academic Press Inc., New York, 1967), p. 305.
[7] D. R. Gustafson, A. R. Mackintosh, and D. J. Zaffarano, Phys. Rev. **130**, 1455 (1963).
[8] D. R. Gustafson and A. R. Mackintosh, Phys. Letters **5**, 234 (1963).
[9] W. Brandt and H. F. Waung, Phys. Letters **27A**, 700 (1968).
[10] S. Berko, S. Cushner, and J. C. Erskine, Phys. Letters **27A**, 668 (1968).
[11] Kunio Fujiwara and Osamu Sueoka, J. Phys. Soc. Japan **23**, 1242 (1967).
[12] J. C. Erskine and J. D. McGervey, Phys. Rev. **151**, 615 (1966).
[13] S. Berko, Phys. Rev. **128**, 2166 (1962).
[14] A. T. Stewart, J. B. Shand, J. J. Donaghy, and J. H. Kusmiss, Phys. Rev. **128**, 118 (1962).
[15] S. Berko and J. S. Plaskett, Phys. Rev. **122**, 1877 (1958).
[16] A. T. Stewart, Can. J. Phys. **35**, 168 (1957).
[17] A. T. Stewart, J. B. Shand, and S. M. Kim, Proc. Phys. Soc. (London) **88**, 1001 (1966).
[18] P. G. Varlashkin (unpublished).

between the detectors. With this geometry, the length of the slits subtends a sufficient angle to allow the customary infinite-slit approximation. Positrons were obtained from a 25 mCi Na^{22} source sealed in stainless steel. The positrons left the sealed source via a thin stainless-steel window. The source was mounted approximately $\frac{1}{2}$ in. above the surface of the alkali metal target. Adjacent lead slits were provided to ensure that photons from annihilations in the source itself, as well as the 1.28-MeV prompt γ ray from the production process, did not reach the detector slits. The source of positrons as well as the annihilation target were mounted between the poles of a magnet which provided a field of 7000 G. The focusing effect of the magnetic field upon the positrons served to enhance the counting rate as well as to prevent annihilations in the walls of the containing vessel. One cesium run (−93°C) was made with a detector slit width of 0.050 in. while all the remaining metal runs were made with a slit width of 0.150 in. The maximum number of coincidence counts recorded per point was 14 000 for the −93°C cesium data run, while all other metal runs ranged from 16 000 to 40 000 coincidence counts at the highest point.

Krypton and xenon were measured using a detector slit width of 0.100 in. The maximum number of counts recorded per point was 12 500 for krypton and 2 500 for xenon. Both of the inert elements were measured in zero magnetic field, and a special mask was provided to prevent positrons from striking the walls of the containing vessel. The inert elements were measured using a Cu^{64} positron source (thin irradiated copper foil). Decay correction was made to compensate for the short half-life of this radioisotope.

Rubidium was measured at −168, −54, 34, and 43°C (molten). Cesium was measured at −172, −93, 6, 16, 31, and 35°C (molten). The metals were vacuum distilled into a stainless-steel measurement cell and continuously vacuum pumped during the data runs. Temperature was cycled from the lowest temperature up into the molten region and then backdown in temperature to check against the possibility of surface oxidation. The entire momentum distribution was scanned repeatedly, each data scan lasting about 3 h. Comparison of each data scan with its predecessor served as a natural check to ensure that the characteristics of the sample had not changed from one scan to the next.

The data have been corrected for instrumental resolution due to slit width and also for positron temperature. After Kim[19] and Garg,[20] the relative effective mass of the positrons was taken as 2.4 in rubidium and 2.6 in cesium. The general procedure for correcting for various resolution functions has been reported in part in Refs. 17, 21, and 22, while more detailed treatments are given in Refs. 23 and 24. Basically, the procedure consists of integrating the product of the resolution function and a trial function (corrected distribution) and comparing the resultant distribution with the experimental results. The trial function is then modified and the procedure repeated until satisfactory agreement is reached. The trial function which produces agreement with experimental results is of course not unique. The procedure is meaningful only as long as no change in curvature is included in the trial function that is not visible in the experimental distribution.

We have devised a resolution correction procedure which we feel is especially useful when the resolution correction is small. The experimental data is used as the trial function and the convolution integral computed. The difference between the integral and the experimental distribution was subtracted from the experimental distribution and the result used as the trial function. In all cases, the convolution of this second trial function produced excellent agreement (to within about four significant figures) with the experimental distribution. Integration was performed numerically using an IBM 360 electronic computer. Comparison of our resolution corrected data with the uncorrected data showed that resolution correction typically did not alter the angular correlation curve by as much as 3%. The most pronounced effect of instrument resolution is to broaden the measured curvature in the vicinity of the Fermi cutoff.

DATA AND DISCUSSION

In Figs. 1 and 2 the left-hand column represents data from which the core contribution has not been subtracted, while the right-hand column shows the results after core subtraction. The solid krypton (−166°C) and xenon (−121°C) cores are shown as dotted lines in the coincidence counting rate distributions of Figs. 1 and 2, respectively. Solid rubidium and cesium are illustrated at two different temperatures in order to show that elevation of the temperature close to the melting point produces no significant effect. The actual data points are shown in the coincidence counting rate distributions with core included. The points on the remainder of the distributions are "synthetic" in that they have been taken from a smooth curve fit to the data. Whenever possible, an electronic computer was used to fit a curve generated from the sum of four Gaussians. The computer generated curve reproduced all the experimental points of the distributions within

[19] S. M. Kim and A. T. Stewart, Bull. Am. Phys. Soc. **12**, 532 (1967).
[20] J. C. Garg and B. L. Saraf, J. Phys. Soc. Japan **25**, 1736 (1968).
[21] P. Colombino, B. Fiscella, and L. Trossi, Nuovo Cimento **38**, 707 (1965).
[22] S. M. Kim and A. T. Stewart, Phys. Rev. Letters **18**, 385 (1967).
[23] S. M. Kim, Ph.D. dissertation, University of North Carolina at Chapel Hill, 1967 (unpublished).
[24] J. A. Arias-Limonta, Ph.D. dissertation, Louisiana State University, 1969 (unpublished).

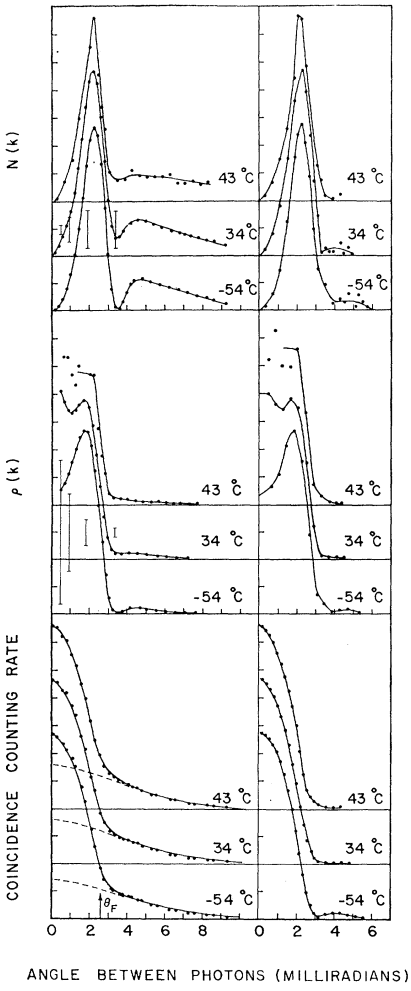

FIG. 1. Electron momentum configuration in liquid and solid rubidium as obtained from positron-annihilation angular correlation. The left-hand column shows the distributions obtained with the contribution from core annihilations included, whereas the right-hand column shows the resultant distributions after core annihilations as determined by a fit to krypton (dotted line) have been removed. θ_F denotes the angle corresponding to the free-electron Fermi momentum. The melting temperature of rubdium is 38.5°C.

less than 0.1% deviation for each individual point. For Rb at 43°C, and for Cs at 16 and 35°C it was not found possible to obtain an adequate computer generated data fit and these were analyzed graphically. Error bars two standard deviations long have been computed for a typical data run as a function of θ. They represent the statistical error that could be anticipated if differentiation of the coincidence counting rate had been obtained by taking the difference between successive data points. Since $\rho(k)$ is obtained by dividing the derivative by θ, the error bars become infinite for sufficiently small θ. The variation in $\rho(k)$ below about 2 mrad comes from minute systematic errors in curve fitting and should not be considered physically significant. Note the disappearance upon removing the core of the high-momentum components [particularly noticeable in the $N(k)$ distributions]. The slight residual amplitude after core removal may indeed be due to higher momentum components of the conduction electrons but is more probably due to the fact that krypton and xenon cannot be expected to exactly duplicate the core distributions of rubidium and cesium.

Since in most metals experimental data on core contribution is not available, core contribution is sometimes obtained from a theoretical calculation; or, as is more often the case, in the absence of a theoretical treatment, simply by fitting the high-momentum portion of the curve to a Gaussian distribution (see for example Refs. 5 and 7). McGervey[6] has pointed out the errors which may be inherent in a Gaussian fit to the core contribution. Figures 3 and 4 show expanded plots

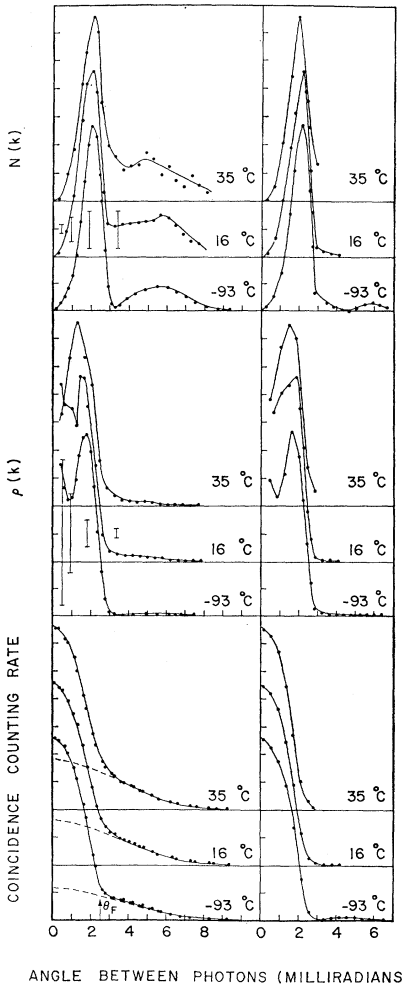

FIG. 2. Electron momentum configuration in liquid and solid cesium as obtained from positron-annihilation angular correlation. The left-hand column shows the distributions obtained with the contribution from core annihilations included, whereas the right-hand column shows the resultant distributions after core annihilation as determined by a fit to xenon (dotted line) have been removed. θ_F denotes the angle corresponding to the free-electron Fermi momentum. The melting temperature of cesium is 28.5°C.

of the high-momentum contribution of rubidium and cesium together with a Gaussian fit to the data and also with krypton and xenon fit to the data. Over the range in which the distributions overlap, the agreement is remarkably close. Note that the amplitude of the Gaussian is too high in the vicinity of low momenta and that this discrepancy diminishes with increasing temperature. This is probably due to the increased disorder at higher temperatures. The change in agreement between the Gaussian and the krypton fits takes place predominantly between −54 and 34°C, while the change between the Gaussian and the xenon fits takes place over the relatively narrow range from 6 to 16°C. Thus, like Al, Cd, In, Pb, and Zn,[2] Rb and Cs change their core angular correlation results below the melting temperature and undergo little further change upon melting. For comparison purposes, the ratios of narrow- to-broad components as determined both by Gaussian and by inert-element fits are tabulated in Tables I and II.

Rubidium shows a decrease in the narrow component upon heating and little change upon melting. Except at the lowest temperature, cesium shows a similar trend. The decrease in the narrow component upon heating is contrary to that generally observed in other metals (see for example, Refs. 1, 2, 25). Further, the absence of significant change in the ratio of the narrow to broad components upon melting is somewhat unusual. Generally, melting enhances the relative size of the narrow component.[1,2,5,7,8]

The slopes of the angular correlation distributions after core removal are shown in Fig. 5 for liquid and

TABLE I. Rubidium. K denotes the percentage narrow component using a krypton core, and G denotes the percentage narrow component as determined with a Gaussian core fit to the data.

Temp (°C)	Phase	% narrow component K	% narrow component G
−168	solid	67	64
−54	solid	63	56
34	solid	55	55
43	liquid	57	56

TABLE II. Cesium. Xe denotes the percentage narrow component using a xenon core, and G denotes the percentage narrow component as determined with a Gaussian core fit to the data.

Temp (°C)	Phase	% narrow component Xe	% narrow component G
−172	solid	60	56
−93	solid	67	61
6	solid	60	56
16	solid	52	54
31	liquid	52	54
35	liquid	49	50

[25] J. H. Kusmiss and J. W. Swanson, Phys. Letters 27A, 517 (1968).

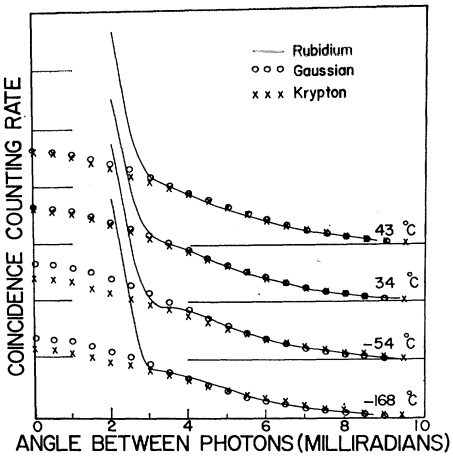

FIG. 3. Distribution of the coincidence counting rate versus angle between photons from positrons annihilating in rubidium and krypton compared with a Gaussian. Frozen krypton was measured at −166°C.

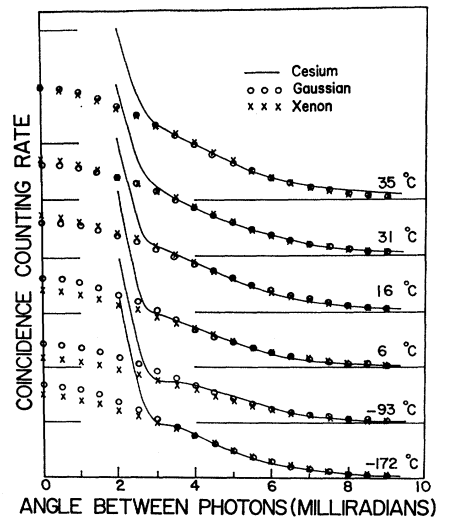

FIG. 4. Distribution of the coincidence counting rate versus angle between photons from positrons annihilating in cesium and xenon as compared with a Gaussian. Frozen xenon was measured at −121°C.

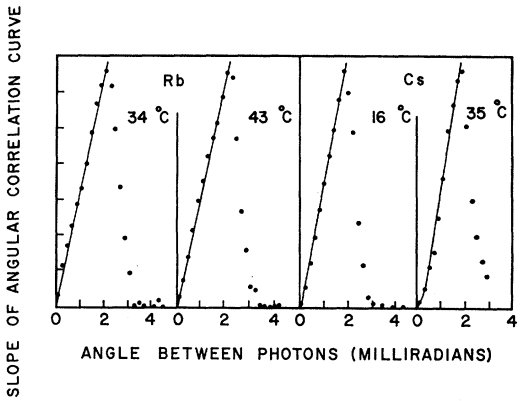

FIG. 5. Slopes of the angular correlation distributions from positrons annihilating in liquid and solid rubidium and cesium.

solid rubidium and cesium. A free-electron momentum distribution in the absence of electron-positron interaction (such as momentum dependence of the annihilation rate) produces a parabolic angular correlation distribution which in turn gives rise to a linear derivative. It is, of course, possible that the momentum enhancement predicted by Kahana and Carbotte[26,27] is present and is masked by a compensating effect. Note that melting produces little or no change in the slopes and the metals retain their free-electron appearance even when molten.

In conclusion, it seems most likely that the vast majority of the higher-momentum components of rubidium and cesium should not be attributed to electrons scattered into the second zone, but are in actuality due to annihilations with core electrons. Second, (assuming that Kr and Xe are accurate core distributions for Rb and Cs) core removal by fitting of a Gaussian curve to the broad component of rubidium and cesium introduces only minor errors in the determination of the ratio of the narrow to broad component, since for these elements a Gaussian distribution approximates the core rather well. Third, the ratio of narrow to broad component is not significantly changed by melting. Fourth, in contrast to more complicated metals, at least for these simple metals, the free-electron model appears to give an adequate representation of the molten state.

[26] S. Kahana, Phys. Rev. **129**, 1622 (1963).
[27] J. P. Carbotte and S. Kahana, Phys. Rev. **139**, A213 (1965).

PHYSICAL REVIEW B VOLUME 1, NUMBER 1 1 JANUARY 1970

Nuclear Magnetic Resonance of ^{57}Fe in the Paramagnetic Alloys $TiFe_{1-x}Co_x$

J. C. SWARTZ,* L. J. SWARTZENDRUBER, AND L. H. BENNETT
Institute for Materials Research, National Bureau of Standards, Gaithersburg, Maryland 20760

AND

R. E. WATSON†
Brookhaven National Laboratory,‡ Upton, New York 11973

(Received 16 July 1969; revised manuscript received 2 September 1969)

Nuclear magnetic resonances (NMR) of ^{57}Fe in isotopically enriched specimens of TiFe, $TiFe_{0.8}Co_{0.2}$, and $FeCl_3$, and of Ti in TiCo are reported. The results supplement existing Fe Mössbauer and Co NMR information on the pseudobinary $TiFe_{1-x}Co_x$. The Knight shift (and estimated uncertainty) of iron in TiFe is $+(1.29\pm0.03)\%$ at room temperature and $+(1.34\pm0.03)\%$ at 77 K, yielding a hyperfine coupling constant of $+(3\pm2)$ kG/μ_B per formula unit. Similar values are obtained for iron in $TiFe_{0.8}Co_{0.2}$. The Knight shift of Ti in TiCo is $+(0.07\pm0.02)\%$ at room temperature, and $-(0.06\pm0.03)\%$ at 77 K, yielding a hyperfine coupling constant of $-(12\pm3)$ kG/μ_B per formula unit for Ti in TiCo, contrasting with a near-zero coupling constant for Ti in TiFe. Both the orbital shifts and the *d*-spin hyperfine coupling constants for the Fe and Ti sites are much less dependent on cobalt concentration than these same quantities at the cobalt site. The NMR results on the three constituents of $TiFe_{1-x}Co_x$ suggest: (i) *s-d* admixture in the wave-function character at the Fermi surface for the (Fe,Co) sublattice, (ii) greater *s* admixture and perhaps a greater *d*-spin moment at an iron site than at a cobalt site in the iron-rich compounds, and (iii) a nuclear moment for cobalt corresponding to a nuclear gryomagnetic ratio $\gamma=2\pi\times1.003$ kHz/G. The Knight shift of dilute Fe in Ti as measured by the Mössbauer effect is $(0\pm1)\%$. The chemical shift of Fe in enriched aqueous $FeCl_3$ is found by NMR to be $+(0.40\pm0.04)\%$.

I. INTRODUCTION

WE have observed the nuclear magnetic resonance (NMR) of ^{57}Fe in enriched samples of intermetallic TiFe, $TiFe_{0.8}Co_{0.2}$, and aqueous $FeCl_3$. These constitute the first NMR observations of ^{57}Fe in any nonferromagnetic material. The experiments were undertaken as part of a continuing study of $TiFe_{1-x}Co_x$ by NMR and Mössbauer-effect (ME) measurements.[1–3]

TiFe and TiCo, each having the CsCl structure, form a complete series of solid solutions with no evidence of crystallographic order on the (Fe,Co) sublattice.[2,4] The

* Research Associate (September 1968–May 1969) at National Bureau of Standards, supported by U. S. Steel Corporation.
† Also consultant, National Bureau of Standards.
‡ Supported by U. S. Atomic Energy Commission.

[1] L. H. Bennett, L. J. Swartzendruber, and R. E. Watson, Phys. Rev. **165**, 500 (1968).
[2] L. J. Swartzendruber and L. H. Bennett, J. Appl. Phys. **39**, 2215 (1968).
[3] L. H. Bennett and L. J. Swartzendruber, Phys. Letters **24A**, 359 (1967).
[4] S. J. Pickart, R. Nathans, and F. Menzinger, J. Appl. Phys. **39**, 2221 (1968).